Decolorization of anthraquinone dye Reactive Blue 4 by natural manganese mineral

Jun Zhai[a,*], Quanfeng Wang[a], Jinsong Zou[b], Kunping Wang[a], Haiwen Xiao[a], Zejin Huang[a], Md. Hasibur Rahaman[a], Alphonse Habineza[a]

[a]College of Urban Construction and Environmental Engineering, Chongqing University, Key Laboratory of the Three Gorges Reservoir Region's Eco-Environment, Chongqing 400045, China, Tel. +86-23-65120750; Mob. 0086-13637966883; Fax: +86-23-65120750; emails: zhaijun@cqu.edu.cn (J. Zhai), 18046504243@163.com (Q. Wang), 957311057@qq.com (K. Wang), xiaohaiwen99@163.com (H. Xiao), 291295998@qq.com (Z. Huang), hasib_esrm@hotmail.com (M.H. Rahaman), habinezaalphonse515@yahoo.com (A. Habineza)
[b]Chongqing CPDI Municipal Engineering Co. Ltd., Chongqing 401147, China, email: 15621699@qq.com

ABSTRACT

Synthetic dye, a valuable industrial material, causes serious pollution to the aquatic environment during manufacture and usage with wastewater discharge. Reactive Blue 4 (RB4), a commercially important anthraquinone dye, was used as the target compound for an experimental investigation on the decolorizating performance of natural manganese mineral. The kinetics of RB4 removal on the surface of natural manganese mineral and its influencing factors and metabolic pathways were studied based on batch experiments. Results demonstrated that the applied natural manganese mineral exhibits an apparently oxidative capacity to transform RB4 with 88.0% ± 1.3% removal efficiency within 24 h. The removal of RB4 mainly resulted from chemical transformation rather than physical adsorption and followed a pseudo-first-order kinetic model. The RB4 degradation was impaired by coexisting metal ions (Fe^{2+} and Mn^{2+}) and an organic reducer (hydroxylamine hydrochloride). The same concentration of Fe^{2+} and Mn^{2+} (0.02 mM) had similar inhibitory effects on the oxidative reactions, and hydroxylamine hydrochloride manifested even greater suppressive effects on the reactions than did Fe^{2+} and Mn^{2+}. A tentative pathway of RB4 degradation by manganese mineral was proposed based on the infrared spectrum results and confirmed by liquid chromatography tandem–mass spectrometry (LC–MS) analysis of RB4 degradation products. This paper suggests that the natural manganese mineral has the potential to be an efficient material for anthraquinone dye removal from natural water or wastewater.

Keywords: Anthraquinone dye; Reactive Blue 4; Natural manganese mineral; Degradation kinetics; Oxidative pathway

1. Introduction

Synthetic dyes, a major class of highly stable organic compounds, are popularly applied in the industries of paper, leather, cosmetics, plastics, clothing, drugs, electronics, and printing [1]. However, around 15% of synthetic dyes are lost directly into wastewater and pose pollution problems in the form of colored wastewater discharged into the aquatic environment [2]. Synthetic organic dyes can also be highly toxic and potentially carcinogenic and mutagenic to the exposed organisms [3,4]. Therefore, the removal of these pollutants from wastewater has become increasingly important.

A range of physical and/or chemical methods, such as coagulation and flocculation [5], adsorption [6], membrane processes [7,8], and advanced oxidation [9,10], has been extensively investigated for the removal of synthetic dyes from aqueous effluents. However, the applications of some above-mentioned methods are still limited because of their

* Corresponding author.

high operational cost [11–14]. Although biological treatment is often deemed an economical alternative in comparison with physical or chemical processes, conventional biological treatment processes are mostly ineffective against dyes [10,15]. Thus, cost-efficient techniques for removing dye from water still require urgent attention.

Manganese dioxides readily participate in a wide variety of environmental redox reactions with reducing potentials of 1.23 V [16]. Manganese oxides can be used for oxidizing different types of inorganic contaminants and organic compounds [16–22]. For instance, Zhang et al. [16,18] demonstrated in their experiment that triclosan and chlorophene can be rapidly oxidized by δ-MnO_2 and developed a kinetic model to quantitatively evaluate the oxidative transformation of organic contaminants. In addition, Lin et al. [20] experimentally showed that δ-MnO_2 has efficient capacity to remove bisphenol A (BPA). In general, the reaction of MnO_2 with organic compounds can be separated into three steps: organic contaminants form complexes with MnO_2; electrons are transferred to MnO_2; and finally, the products dissociate from MnO_2 [20,23]. However, most of the studies investigated the removal of organic contaminants using synthetic pure manganese oxides, while studies on the oxidation of organic pollutants by natural manganese mineral as an alternative method remain limited.

Minerals containing Mn(III) and Mn(IV) are potential oxidizing agents for both natural and xenobiotic organic compounds [24]. With their large surface areas and high chemical activity, the manganese minerals are involved in a wide variety of oxidation–reduction and cation-exchange reactions [25]. Natural manganese minerals containing Mn(IV) are abundant in China [26], and their potential use as media to remove synthetic dyes will support a cost-effective treatment method to minimize the pollution of the aquatic environment. In this regard, the current study uses a commercially important anthraquinone dye, Reactive Blue 4 (RB4) as the target compound. The molecular formula and molar mass of RB4 are $C_{23}H_{14}Cl_2N_6O_8S_2$ and 637.43 g/mol, respectively, and its molecular structure is shown in Fig. 1. The main objectives of this study are to assess the decolorization of RB4 at the manganese mineral surface, to discuss the impact of the presence of Fe^{2+} and Mn^{2+} and an organic reducer (hydroxylamine hydrochloride), and to investigate the metabolic pathways of RB4.
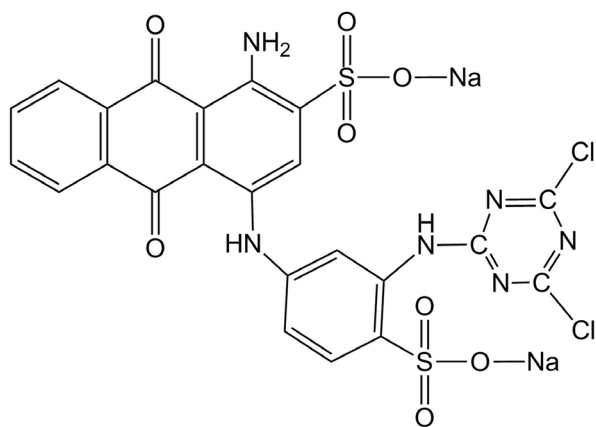
2. Materials and methods

2.1. Chemicals and reagents

RB4 (CAS No. 13324-20-4) with a reported purity >99% was purchased from Sigma-Aldrich (St. Louis, MO, USA). Spectral pure grade KBr was purchased from Guangfu Chemical (Tianjin, China). Reagent water (18.2 MΩ resistivity) was prepared using a Millipore Milli-Q water purification system (Millipore S.A.S, Merck, Germany). The dye's stock solution (400 mgL^{-1}) was prepared with the reagent water and stored in a 4°C freezer without light prior to use.

2.2. Preparation and characterization of natural manganese mineral

The natural manganese mineral was collected from Hebei Province, China, then treated by ultrasonic cleaning, drying, and crushing sieving to a particle size 0.25–2 mm prior to use. Powder X-ray diffraction (XRD) analysis was carried out on a Rigaku diffractometer, model D/MAX-III, to determine the crystal phase and structure of the manganese mineral. Diffraction patterns of the samples were recorded with Cu kα radiation and recorded in the range of 10.0°–90.0° with a scanning rate of 2.0°/min and a step size of 0.02°. The X-ray tube was operated at 40 kV and 80 mA. X-ray fluorescence (XRF) analysis was performed through the XRF analyzer (PPM-100%, BAIRD, Co., USA) to investigate the element composition of the natural manganese mineral. The manganese mineral particles were dried in nitrogen gas and powdered in an agate bowl before analysis. Samples for XRF analysis were prepared according to the method used by a previous study [27].

2.3. Reaction setup

Experiments were conducted in 1,000 mL glass conical flasks under ambient O_2 conditions. Reaction solutions (500 mL) were constantly mixed by horizontal shaking at 25°C ± 1°C and 200 rpm in an oscillator (SKY-2102C). Five reactors with different material compositions were set up to evaluate the decolorization of RB4 by the natural manganese mineral and investigate the effects of metal ions, including Fe^{2+} and Mn^{2+} and the organic reducer (hydroxylamine hydrochloride) on RB4 degradation by manganese

Fig. 1. Molecular structure of the RB4.

Table 1
Material composition of the five experimental reactors

Reaction reactor	Material composition
Reactor A (as control)	200 mgL^{-1} RB4
Reactor B	20 g manganese mineral, 200 mgL^{-1} RB4
Reactor C	20 g manganese mineral, 200 mgL^{-1} RB4 and 0.02 mM Fe^{2+}
Reactor D	20 g manganese mineral, 200 mgL^{-1} RB4 and 0.02 mM Mn^{2+}
Reactor E	20 g manganese mineral, 200 mgL^{-1} RB4 and 0.2 M hydroxylamine hydrochloride

Note: The total volume of reaction solution in all reactors is 500 mL.

mineral (Table 1). Reactions were initiated by adding 500 mL of a 200 mg L^{-1} RB4 solution to the 1,000 mL conical flasks. Aliquots of reaction mixture in each reactor were periodically withdrawn at 0, 2, 4, 6, 8, 10, 12, 14, 16, 18, 20, 22, and 24 h intervals, respectively. Subsequently, the suspension was separated by syringe filtration through 0.45 μm nylon filters. The filtrate was then used to measure the concentration of RB4 and Mn^{2+} and determine the total carbon (TC), total organic carbon (TOC), and total inorganic carbon (TIC). In addition, the filtrate collected from reactor B at certain intervals was used to conduct UV-Vis full wavelength scan, infrared spectroscopy, and liquid chromatography tandem–mass spectrometry (LC–MS) analysis to determine the RB4 degradation products. Meanwhile, to determine the quantity of RB4 adsorbed on the surface of manganese minerals, desorption experiments were conducted for the separated manganese minerals collected from reactor B. The separated manganese minerals were dried by nitrogen gas and then immersed in 200 mL Milli-Q water after weighing. The released RB4 concentrations were measured after 30 min shaking (300 rpm, 25°C ± 1°C), to calculate the quantity of RB4 adsorbed on the surface of manganese minerals. All the experiments were performed in triplicate.

2.4. Kinetic calculation

To examine the reaction kinetics of the RB4 transformation by manganese minerals, the data of RB4 concentrations in the reaction solutions over time were fitted to the pseudo-first-order kinetic model [22,23] given in Eqs. (1) and (2):

$$C_t = C_0 e^{-kt} \tag{1}$$

The logarithmic form of Eq. (1) is as follows:

$$\ln(C_t) = -kt + \ln(C_0) \tag{2}$$

where C_0 (mgL^{-1}) and C_t (mgL^{-1}) are RB4 concentrations at time 0 and an elapsed time t, respectively, and k (h^{-1}) is the pseudo-first-order rate constant. When the Napierian logarithm (ln) of RB4 concentrations was plotted against time, the slopes of the linearized curve represent the pseudo-first-order rate constant k (h^{-1}).

2.5. Analysis methods

The RB4 concentration for each time was determined by UV-Vis spectrophotometry, at wavelength λ = 597 nm, which corresponds to the maximum absorbance for RB4 [16]. The Mn^{2+} concentration in the filtrate was analyzed by atomic absorption spectroscopy (AAS; TAS-990AFG, PERSEE). The TC/TOC and TC were measured by a TOC analyzer named Perkin-Elmer Lambda 90. The full wavelength scan was performed through an UV-Vis spectrophotometer (model UV2450) from Shimadzu, Japan. Infrared spectra were collected from 400 to 4,000 cm^{-1} using a Perkin-Elmer Lambda 90 spectrometer. The samples for infrared spectroscopic analysis were prepared through the method used by Chen [17]. The resolution for the infrared spectra was set at 4.0 cm^{-1}, and 64 scans were collected for each spectrum. Reaction products of RB4 were

analyzed by an high performance liquid chromatography–mass spectrometry (HPLC–MS) system with a Zorbax SB-C18 column (2.4 × 150 mm, 5 μm) (1200/6100MSD, Agilent Technology, USA. . The column was maintained at room temperature. The injection volume was 20 μL, and the eluent flow rate was 0.20 mL/min. The MS analysis was conducted by electrospray positive ionization at the fragmentation voltage 80–120 V with mass scan range 50–1,000 m/z. Other LC–MS instrumental parameters were similar to those previously reported [28].

2.6. Statistical analysis

Two-way analysis of variance (ANOVA) and Fisher's least significant difference (LSD) *post hoc* (α = 0.05) tests were used to determine the significant differences between the RB4 removal efficiencies in different experimental reactors. The two factors for the two-way ANOVA were reaction time and different treatment reactors where samples were collected. Pearson correlation coefficients at the 95% confidence level between ln of RB4 concentrations and reaction time were analyzed to judge the reaction kinetics of RB4 transformation by manganese mineral. The calculations were carried out with Origin 9.0 software.

3. Results and discussion

3.1. Manganese mineral characterization

Results from the XRD pattern of the studied manganese mineral showed diffraction peaks of rancieite [(Ca, Mn^{2+}) Mn$^{4+}_4$ O$_9$ • 3H$_2$O], johannsenite (CaMn^{2+} Si$_2$O$_6$), dolomite [CaMg(CO$_3$)$_2$], and quartz crystal (SiO$_2$) (Fig. 2), all of which indicated the existence of these mineral components in the investigated mineral. The elemental composition of the natural manganese mineral is summarized in Table 2. The most abundant metal element in the studied mineral is Mn (8.27%), followed by K, Al, Ca, Fe, and Mg, which account for 6.00%, 5.65%, 5.57%, 3.92%, and 1.88% of the elemental composition, respectively. The percentage of Si element is 23.76% among all elements. Combined with XRD analysis, the results show that the studied manganese minerals contain less manganese oxides than the implemented mineral by Liu and Tang [26], which had a Mn percentage of 30.6%.
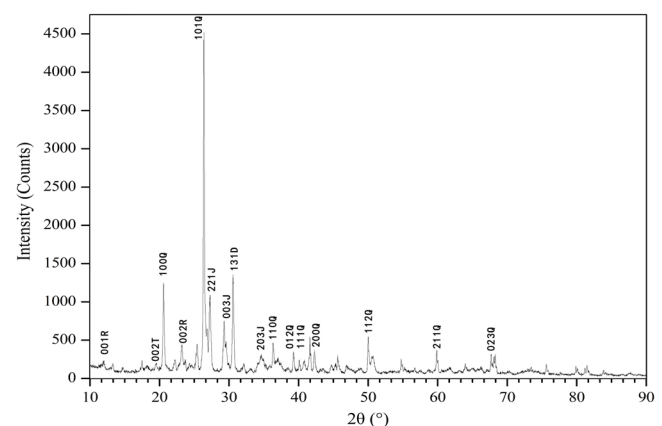

Fig. 2. XRD pattern of the manganese mineral (Q: Quartz; R: Rancieite; J: Johannsenite; and D: dolomite).

3.2. Degradation of RB4

In the absence of manganese mineral, RB4 concentration was stable under the experimental conditions, and no evident removal of RB4 was detected (Fig. 3(a), reactor A). By contrast, significant degradation of RB4 occurred in the presence of manganese mineral, and the maximum degradation rate of RB4 reached $88.0\% \pm 1.3\%$ after 24 h in reactor B, which contained 20 g of the studied manganese mineral and 500 mL of a 200 mg L^{-1} RB4 solution. On the basis of the desorption experiment, the removal rate of RB4 due to adsorption was accounted for less than $1.2\% \pm 0.2\%$ of the total RB4 removal in the reaction solution of reactor B (data not shown). Our findings suggested that the disappearance of RB4 in the reaction solution mainly resulted from chemical transformation rather than physical adsorption on the surfaces of the natural manganese mineral.

This study also investigated the degradation effect of RB4 by natural manganese mineral amended with metal ions (Fe^{2+} and Mn^{2+} of both 0.02 mM) and an organic reducer (0.2 M hydroxylamine hydrochloride). The removal efficiencies of RB4 were found to be $84.6\% \pm 1.0\%$, $85.5\% \pm 0.8\%$, and 76.5% $\pm 0.7\%$ in reactors C, D and E, respectively, after a 24-h reaction time. The concentrations of RB4 in reactor B based on the results from two-way ANOVA at various sampling times were significantly lower than the concentrations in reactors C, D, and E ($P < 0.05$), indicating that the presence of Mn^{2+}, Fe^{2+}, and hydroxylamine hydrochloride had an inhibitory effect on RB4 degradation by the manganese mineral. The RB4 concentration in reactor E at different sampling times was also significantly higher than the concentrations in reactors C and D ($P < 0.05$), while the RB4 concentrations in reactors C and D were comparable with each other ($P > 0.05$). Our results suggested that the same concentrations of Fe^{2+} and Mn^{2+} show similar inhibitory effects for RB4 oxidation, whereas hydroxylamine hydrochloride manifests even greater suppressive effects on the degradation reaction than the studied metal ions.

The coexisting metal ions could inhibit the reaction of manganese oxide with organic contaminants through the decrease of available active surface sites with the occupation of oxide surface sites by co-solutes [18,20,23]. Furthermore, the presence of dissolved organic matters (DOM) could suppress the oxidation reaction by providing an alternate source of negatively charged binding sites, blocking MnO_2 reactive sites, and reacting with MnO_2, which enhances the dissolution of MnO_2 [18,29]. The concentration of Mn^{2+} in different reactors over time is illustrated in Fig. 3(b). The concentration of Mn^{2+} in all reactors shows a trend of increasing first and subsequently reducing to zero. This initial increase of Mn^{2+} implies that Mn^{2+} was produced through dissolution of manganese mineral and disappeared through adsorption by the manganese mineral. However, the addition of Fe^{2+}, Mn^{2+}, and hydroxylamine hydrochloride has different degrees of influence on the peak value of Mn^{2+} concentration. Therefore, the results of this study indicate that the same concentrations of Fe^{2+} and Mn^{2+} (0.02 mM) having a similar affinity with the surface sites of manganese mineral and hydroxylamine hydrochloride could occupy the manganese mineral surface reactive sites and react with manganese mineral. Such

Table 2
Elemental composition of the studied natural manganese mineral

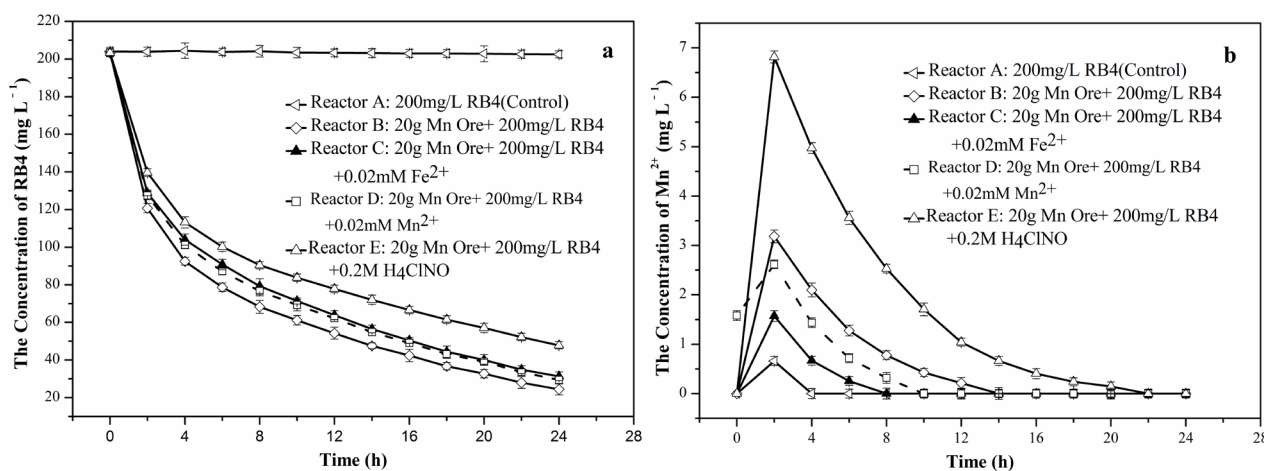| Elements	Percentage (%)
O	44.39
Si	23.76
Mn	8.27
K	6.00
Al	5.65
Ca	5.57
Fe	3.92
Mg	1.88
Ti	0.30
P	0.12

Fig. 3. Concentrations of: (a) RB4 and (b) Mn^{2+} as a function of experimental time in reactors A, B, C, D, and E (reactor A only contained 500 mL of a 200 mg L^{-1} RB4 solution; reactors B, C, D, and E contained 500 mL of a 200 mg L^{-1} RB4 solution and 20 g manganese minerals; and reactor C, D, and E also contained 0.02 mM Fe^{2+}, 0.02 mM Mn^{2+}, and 0.2 M hydroxylamine hydrochloride, respectively). Data points are given as means ± standard errors (n = 3).

outcomes thereby result in even greater suppressive effects on RB4 oxidation by the manganese mineral.

Changes of TC, TOC, and TIC in the experimental reactor B over time are shown in Fig. 4. The TOC in the reactor solution decreased from 85.98 ± 0.83 to 64.69 ± 1.30 mgL^{-1}, corresponding to a removal efficiency of 24.76% after 24 h, while the TIC increased from 1.67 ± 0.83 to 22.91 ± 1.05 mgL^{-1} (Fig. 4). The RB4 could be degraded through oxidation at the natural manganese mineral surface and partly mineralized to inorganic compounds. Moreover, the TC basically remained unchanged and maintained balance with the sum of TOC and TIC throughout the reaction time [TC = 90.43 ± 1.46 mgL^{-1}, TC = (TOC + TIC) ± 2.05 mgL^{-1}], thereby indirectly indicating that the RB4 removal caused by adsorption was negligible under the experiment conditions.

In this study, the reaction kinetics of the transformation of RB4 by manganese mineral was investigated. The RB4 concentrations in reactors B, C, D, and E gradually decreased and had a tendency to flatten out with the increase of time (Fig. 3). A general pseudo-first-order kinetics model (Eqs. (1) and (2)) was employed to evaluate the RB4 degradation process. When the ln of RB4 concentrations were plotted against time, linear fits were obtained with correlation coefficients (R^2) 0.95, 0.96, 0.95, and 0.93 for reactors B, C, D, and E, respectively, at the 95% confidence level. This study revealed that the transformation of RB4 in different reactors closely followed the pseudo-first-order kinetic model and the pseudo-first-rate constant k was 0.076, 0.070, 0.068, and 0.051 h^{-1} in reactors B, C, D, and E, respectively. Similar reaction kinetics were also reported in other Mn oxide-mediated reactors for chemical oxidation of organics [22,23]. The difference of rate constant in various experimental reactors likewise indirectly suggested that the presence of Mn^{2+}, Fe^{2+}, and hydroxylamine hydrochloride shows different levels of inhibitory effect on RB4 oxidation, which is in accordance with the results from the two-way ANOVA.

A surface mechanism involving the sorption of organic compounds to the manganese oxide surface and the subsequent electron transfer has been proposed by other researchers [30–32]. 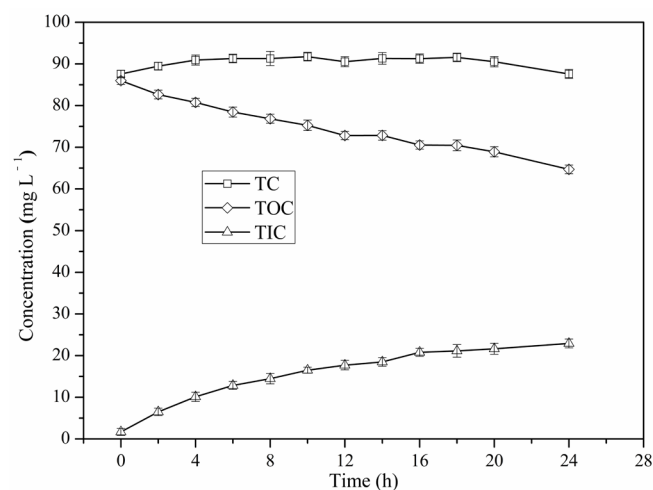The results of the current study suggested that the reaction of RB4 with manganese mineral also follows the similar surface reaction process.

3.3. Proposed reaction pathway of RB4

The result of the UV-Vis full wavelength scan of samples from reactor B is illustrated in Fig. 5. The absorbance at 597, 375, and 281 nm bands related to the anthraquinone group [33,34] evidently decreased with the reaction time. In addition, the peak at 256 nm attributed to the aromatic character and chlorotriazine group [34,35] decreased significantly. This finding indicated that the chromophore components and anthraquinone group of the dye molecules were degraded within the reaction process of RB4 at the natural manganese mineral surface. At the same time, the cleavage of the aromatic and chlorotriazine group structure could also take place.

The infrared spectra of the solution at different reaction times are shown in Fig. 6. In the infrared spectra, the RB4 in the solution at the beginning of reaction (0 h) showed typical peaks at 3,430, 2,600–3,050, 1,723, 1,625, 1,461, 1,401, 1,259, and 1,027, and at 1,149, and 1,119 cm^{-1}. These peaks are attributable, respectively, to the frequencies of N–H stretching [36], aromatic C–H stretching [37], quinone C=O stretching [38], C=N stretching of chlorotriazine [39], C–N bending deformation [40], C=C stretching at aromatic nucleus [41], S=O stretching of sulfonic group [36,37], and C–H bending deformation of benzene ring [27,41]. With the oxidation of RB4 by manganese mineral, the peaks at 1,723 and 1,461 cm^{-1} rapidly decreased and almost disappeared after 4-h reaction time, which indicated that the chemical bonds of C=O and C–N in RB4 molecule were first broken by oxidation of manganese mineral. In addition, a new absorption peak corresponding to C–O stretching of ethers or other carbohydrate [27,40] appeared at 1,200 cm^{-1} within the first 8 h of the reaction time, and then gradually disappeared. The present results suggested that some new matters were produced during the reaction and then oxidized further by manganese mineral. The absorption peak at 1,625, 1,149, and 1,119 cm^{-1} became stronger within the first 8 h of reaction time, and then gradually weakened at

Fig. 4. Variations of TC, TOC, and TIC over the reaction time in reactor B. Data points are given as means ± standard errors (n = 3).
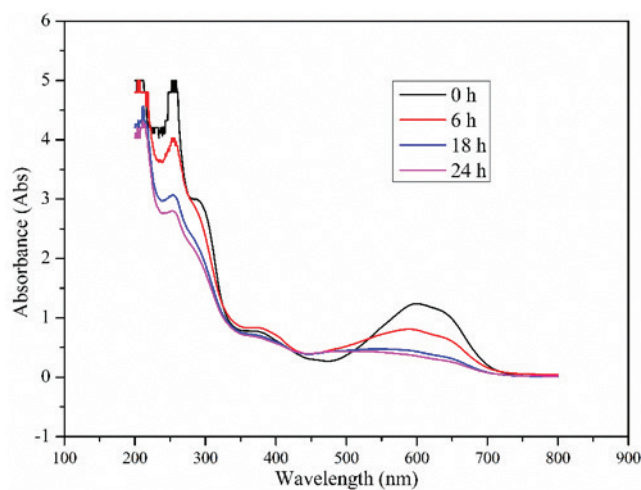
Fig. 5. UV-V is full wavelength scan of RB4 at different reaction times in reactor B.
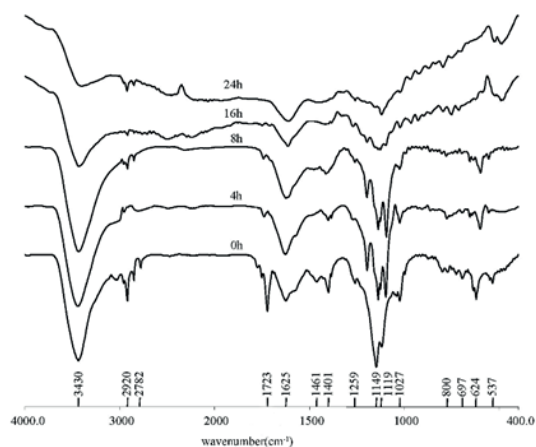
Fig. 6. Infrared spectra of solution at certain times in reactor B.

Fig. 7. LC–MS analysis of the organic intermediates of RB4 after a 4-h treatment in reactor B.

the succeeding 16–24 h of reaction time. These results revealed that the groups of triazine structure and benzene ring were stable within the early period of the reaction, and afterward, a portion of these groups were further destroyed by the oxidation of manganese mineral. The peaks of RB4 observed at 1,259 and 1,027 cm^{-1} gradually decreased and were clearly absent after 24 h of reaction time, indicating that the −SO$_3$H groups in RB4 molecules were detached. The results of infrared spectroscopic analysis indicated that the chromophoric group in molecule RB4 was adequately broken, and a part of the intermediate products were converted into CO$_2$ and H$_2$O. This phenomenon could be supported by the concentrations in the TC, TOC, and TIC results.

Six products were detected by LC–MS analysis and could be the molecular m/z of 123.03, 166.02, 167.38, 190.12, 189.31, and 523.54, respectively. These products were tentatively identified as benzoic acid, 2-amino-4,6-dichlorotriazine, phthalic acid, 2,3-dihydroxy-benzenesulfonic acid, 4-amino-2-hydroxybenzenesulfonic acid, and 5-((3-((4,6-dichloro-1,3,5-triazin-2-yl)amino)-4-sulfonatophenyl)amino)-2,3-dihydroxybenzenesulfonate, respectively (Fig. 7). Similar intermediate compounds were also formed by using a marine fungus to degrade RB4, as studied by Verma et al. [42]. In their study, 1,000 mgL^{-1} of RB4 treated with partially purified laccase of the marine-derived fungus resulted in 61% color removal and 47% decrease in chemical oxygen demand in 12 h. The degradation rate of RB4 by the manganese mineral was comparable with this biological treatment method. However, smaller molecular weight compounds were produced in the process of RB4 treatment by the manganese mineral, given that the degradation products could not serve as substrates for the enzyme. Toxicity tests are very important for any bioremediation and chemical remediation process. However, the toxicity assay of RB4 before and after treatment with manganese mineral was not carried out in this work. Given that this study mostly focuses on the removal efficiency of RB4 by natural manganese mineral, the toxicity assay should be taken into consideration in future research.

On the basis of the experimental results of UV-Vis full wavelength scan, infrared spectrum, and LC–MS analysis, this study proposed a degradation pathway of RB4 using
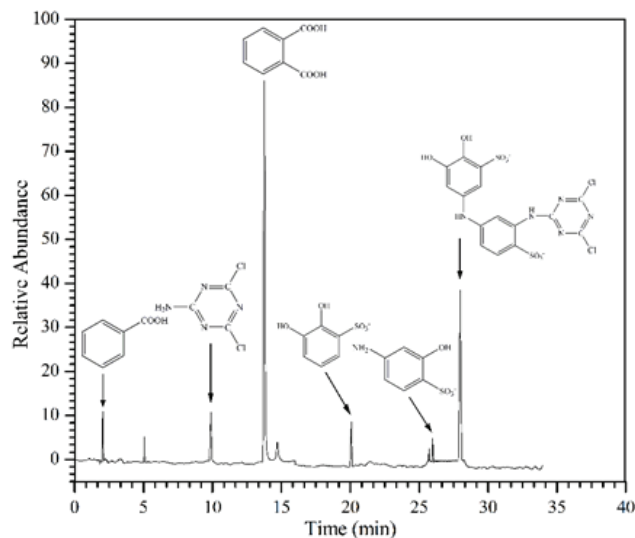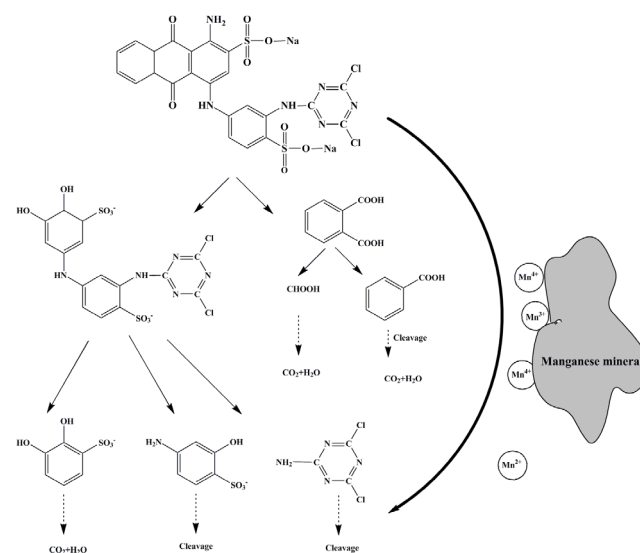

Fig. 8. Proposed oxidation reaction pathway for RB4 degradation by natural manganese minerals.

natural manganese mineral (Fig. 8). For the process of RB4 oxidation on the surface of the studied manganese mineral, first, the C=O double bond of the anthraquinone group and the C–N bond in the molecule RB4 were broken, which caused the molecule RB4 to cleave into phthalic acid. The rest of the RB4 molecules were sequentially attacked and cleaved into 2,3-dihydroxy-benzenesulfonic acid sodium salt, 4-amino-2-hydroxybenzenesulfonic acid sodium salt, and 2-amino-4,6-dichlorotriazine. Thereafter, the phthalic acid cleaved into benzoic acid and oxidated into micromolecule acid or ketone. Finally, different types of benzenesulfonic acid sodium salt with different substituent groups were partly oxidized into CO$_2$ and H$_2$O.

4. Conclusions

This study proved that natural manganese mineral can be effective materials to remove dye compounds in natural water or wastewater. The maximum RB4 removal rate was 88.0% ± 1.3% after a 24-h reaction time under various experimental conditions, and the degradation of RB4 was mostly caused by oxidation by the Mn(IV)/Mn(III) in the natural manganese minerals. The degradation of RB4 at the surface of the natural manganese mineral followed a pseudo-first-order kinetic model. The reaction was impaired by the coexistence of metal ions (Fe^{2+} and Mn^{2+}) and an organic reducer (hydroxylamine hydrochloride). RB4 was partly mineralized with the presence of natural manganese mineral, and the chemical metabolic pathways were proposed based on the infrared spectrum results and confirmed by the LC–MS analysis of RB4 degradation products. This study will improve the understanding on the degradation pathway of dye compounds using natural manganese minerals and its further application in cost-efficient full-scale industrial wastewater treatment.

References

[1] R. Vinu, G. Madras, Kinetics of sonophotocatalytic degradation of anionic dyes with nano-TiO_2, Environ. Sci. Technol., 43 (2009) 473–479.

[2] S.A. Medina-Moreno, R. Perez-Cadena, A. Jimenez-Gonzalez, A. Tellez-Jurado, C.A. Lucho-Constantino, Modeling wastewater biodecolorization with reactive blue 4 in fixed bed bioreactor by Trametes subectypus: biokinetic, biosorption and transport, Bioresour. Technol., 123 (2012) 452–462.

[3] G. Akkaya, A. Ozer, Biosorption of Acid Red 274 (AR 274) on *Dicranella varia*: determination of equilibrium and kinetic model parameters, Process Biochem., 40 (2005) 3559–3568.

[4] P. Kaushik, A. Mishra, A. Malik, K.K. Pant, Biosorption of textile dye by *Aspergillus lentulus* pellets: process optimization and cyclic removal in aerated bioreactor, Water Air Soil Pollut., 225 (2014) 1978. doi:10.1007/s11270-014-1978-x

[5] A.K. Verma, R.R. Dash, P. Bhunia, A review on chemical coagulation/flocculation technologies for removal of colour from textile wastewaters, J. Environ. Manage., 93 (2012) 154–168.

[6] F.R. Furlan, L.G. de Melo da Silva, A.F. Morgado, A.A. Ulson de Souza, S.M.A. Guelli Ulson de Souza, Removal of reactive dyes from aqueous solutions using combined coagulation/flocculation and adsorption on activated carbon, Resour. Conserv. Recycl., 54 (2010) 283–290.

[7] A. Akbari, S. Desclaux, J.C. Rouch, P. Aptel, J.C. Remigy, New UV-photografted nanofiltration membranes for the treatment of colored textile dye effluents, J. Membr. Sci., 286 (2006) 342–350.

[8] R. Huang, B. Yang, D. Zheng, G. Chen, C. Gao, Treatment of textile dye effluent using a self-made positively charged nanofiltration membrane, J. Wuhan Univ. Technol., 27 (2012) 199–202.

[9] B. Gozmen, B. Kayan, A.M. Gizir, A. Hesenov, Oxidative degradations of reactive blue 4 dye by different advanced oxidation methods, J. Hazard. Mater., 168 (2009) 129–136.

[10] M. Becelic-Tomin, B. Dalmacija, L. Rajic, D. Tomasevic, D. Kerkez, M. Watson, A. Prica, Degradation of anthraquinone dye reactive blue 4 in pyrite ash catalyzed Fenton reaction, Scientific World J. (2014) 234654. http://dx.doi.org/10.1155/2014/234654

[11] G. Bayramoglu, G. Celik, M.Y. Arica, Biosorption of Reactive Blue 4 dye by native and treated fungus Phanerocheate chrysosporium: batch and continuous flow system studies, J. Hazard. Mater., 137 (2006) 1689–1697.

[12] Y.H. Lee, S.G. Pavlostathis, Decolorization and toxicity of reactive anthraquinone textile dyes under methanogenic conditions, Water Res., 38 (2004) 1838–1852.

[13] T.R. Waghmode, M.B. Kurade, A.N. Kagalkar, S.P. Govindwar, Differential fate of metabolism of a disperse dye by microorganisms Galactomyces geotrichum and Brevibacillus laterosporus and their consortium GG-BL, J. Environ. Sci. (China), 24 (2012) 1295–1304.

[14] S.P. Govindwar, M.B. Kurade, D.P. Tamboli, A.N. Kabra, P.J. Kim, T.R. Waghmode, Decolorization and degradation of xenobiotic azo dye Reactive Yellow-84A and textile effluent by *Galactomyces geotrichum*, Chemosphere, 109 (2014) 234–238.

[15] W.J. Epolito, H. Yang, L.A. Bottomley, S.G. Pavlostathis, Kinetics of zero-valent iron reductive transformation of the anthraquinone dye Reactive Blue 4, J. Hazard. Mater., 160 (2008) 594–600.

[16] H. Zhang, W. Chen, C. Huang, Kinetic modeling of oxidation of antibacterial agents by manganese oxide, Environ. Sci. Technol., 42 (2008) 5548–5554.

[17] W. Chen, Y. Ding, C.T. Johnston, B.J. Teppen, S.A. Boyd, H. Li, Reaction of lincosamide antibiotics with manganese oxide in aqueous solution, Environ. Sci. Technol., 44 (2010) 4486–4492.

[18] H.C. Zhang, C.H. Huang, Oxidative transformation of triclosan and chlorophene by manganese oxides, Environ. Sci. Technol., 37 (2003) 2421–2430.

[19] K. Lin, W. Liu, J. Gan, Oxidative removal of bisphenol A by manganese dioxide: efficacy, products, and pathways, Environ. Sci. Technol., 43 (2009) 3860–3864.

[20] K. Lin, W. Liu, J. Gan, Reaction of tetrabromobisphenol A (TBBPA) with manganese dioxide: kinetics, products, and pathways, Environ. Sci. Technol., 43 (2009) 4480–4486.

[21] K. Lin, Y. Peng, X. Huang, J. Ding, Transformation of bisphenol A by manganese oxide-coated sand, Environ. Sci. Pollut. Res., 20 (2013) 1461–1467.

[22] Z. Lu, K. Lin, J. Gan, Oxidation of bisphenol F (BPF) by manganese dioxide, Environ. Pollut., 159 (2011) 2546–2551.

[23] A.T. Stone, Reductive dissolution of manganese(III/IV) oxides by substituted phenols, Environ. Sci. Technol., 21 (1987) 979–988.

[24] H.J. Ulrich, A.T. Stone, Oxidation of chlorophenols of adsorbed to manganese oxide surfaces, Environ. Sci. Technol., 23 (1989) 421–428.

[25] J.E. Post, Manganese Oxide Minerals: Crystal Structures and Economic and Environmental Significance, Proc. National Academy of Sciences of the United States of America, Vol. 96, 1999, pp. 3447–3454.

[26] R.X. Liu, H.X. Tang, Oxidative decolorization of direct light red F3B dye at natural manganese mineral surface, Water Res., 34 (2000) 4029–4035.

[27] N.R. Neti, R. Misra, Efficient degradation of Reactive Blue 4 in carbon bed electrochemical reactor, Chem. Eng. J., 184 (2012) 23–32.

[28] W. Epolito, Y. Lee, L. Bottomley, S. Pavlostathis, Characterization of the textile anthraquinone dye Reactive Blue 4, Dyes Pigm., 67 (2005) 35–46.

[29] J. Klausen, S.B. Haderlein, R.P. Schwarzenbach, Oxidation of substituted anilines by aqueous MnO_2: effect of co-solutes on initial and quasi-steady-state kinetics, Environ. Sci. Technol., 31 (1997) 2642–2649.

[30] A.T. Stone, J.J. Morgan, Reduction and dissolution of manganese(III) and manganese(IV) oxides by organics. 1. Reaction with hydroquinone, Environ. Sci. Technol., 18 (1984) 450–456.

[31] A.T. Stone, J.J. Morgan, Reduction and dissolution of manganese(III) and manganese(IV) oxides by organics. 2. Survey of the reactivity of organics, Environ. Sci. Technol., 18 (1984) 617–624.

[32] H.C. Zhang, C.H. Huang, Reactivity and transformation of antibacterial N-oxides in the presence of manganese oxide, Environ. Sci. Technol., 39 (2005) 593–601.

[33] P.A. Carneiro, M.E. Osugi, C.S. Fugivara, N. Boralle, M. Furlan, M. Zanoni, Evaluation of different electrochemical methods on the oxidation and degradation of Reactive Blue 4 in aqueous solution, Chemosphere, 59 (2005) 431–439.

[34] O.B. Ayodele, O.S. Togunwa, Catalytic activity of copper modified bentonite supported ferrioxalate on the aqueous degradation and kinetics of mineralization of Direct Blue 71, Acid Green 25 and Reactive Blue 4 in photo-Fenton process, Appl. Catal., A, 470 (2014) 285–293.

[35] P.A. Carneiro, R.F. Pupo Nogueira, M.V.B. Zanoni, Homogeneous photodegradation of C.I. Reactive Blue 4 using a photo-Fenton process under artificial and solar irradiation, Dyes Pigm., 74 (2007) 127–132.

[36] F.M. Machado, C.P. Bergmann, E.C. Lima, B. Royer, F.E. de Souza, I.M. Jauris, T. Calvete, S.B. Fagan, Adsorption of Reactive Blue 4 dye from water solutions by carbon nanotubes: experiment and theory, Phys. Chem. Chem. Phys., 14 (2012) 11139–11153.

[37] C.S. Martin, M.F.S. Teixeira, Electrocatalytic study of an electrode modified with Reactive Blue 4 dye covalently immobilized on amine-functionalized silica, J. Solid State Electrochem., 16 (2012) 3877–3886.

[38] R. Renjith, Y.S. Mary, H.T. Varghese, C.Y. Panicker, T. Thiemann, C. Van Alsenoy, Vibrational spectra, molecular structure, NBO, HOMO-LUMO and first order hyperpoalarizability analysis of 1,4-bis(4-formylphenyl) anthraquinone by density functional theory, Spectrochim. Acta, 131 (2014) 225–234.

[39] R. Renjith, Y.S. Mary, C.Y. Panicker, H.T. Varghese, M. Pakosinska-Parys, C. Van Alsenoy, T.K. Manojkumar, Spectroscopic (FT-IR, FT-Raman), first order hyperpolarizability, NBO analysis, HOMO and LUMO analysis of 1,7,8,9-tetrachloro-10, 10-dimethoxy-4-[3-(4-phenylpiperazin-l-yl)propyl]-4-azatricyclo $[5.2.1.0^{2,6}]$dec-8-ene-3,5-dione by density functional methods, Spectrochim. Acta, 124 (2014) 500–513.

[40] D.M. Kaminski, A. Matwijczuk, D. Pociecha, E. Gorecka, A. Niewiadomy, M. Dmowska, M. Gagos, Effect of 2-(4-fluoro-phenylamino)-5-(2,4-dihydroxyphenyl)-1,3,4-thiadiazole on the molecular organisation and structural properties of the DPPC lipid multibilayers, Biochim. Biophys. Acta, 1818 (2012) 2850–2859.

[41] Z.M. Hua H. Ping, Instrumental Analysis, 4th ed., Higher Education Press, Beijing, China, 2008, pp. 298–307.

[42] A.K. Verma, C. Raghukumar, R.R. Parvatkar, C.G. Naik, A rapid two-step bioremediation of the anthraquinone dye, Reactive Blue 4 by a marine-derived fungus, Water Air Soil Pollut., 223 (2012) 3499–3509.